



Lawrence Berkeley Laboratory

UNIVERSITY OF CALIFORNIA

Accelerator & Fusion Research Division

Center for X-Ray Optics

Received by OSTI

NOV 25 1986

Presented at the AIP Third Topical Meeting on
Short Wavelength Coherent Radiation: Generation
and Applications, Monterey, CA, March 24-27, 1986;
and to be published in the Proceedings 147, D.T. Attwood
and J. Bokor, Eds., American Institute of Physics, May 1986

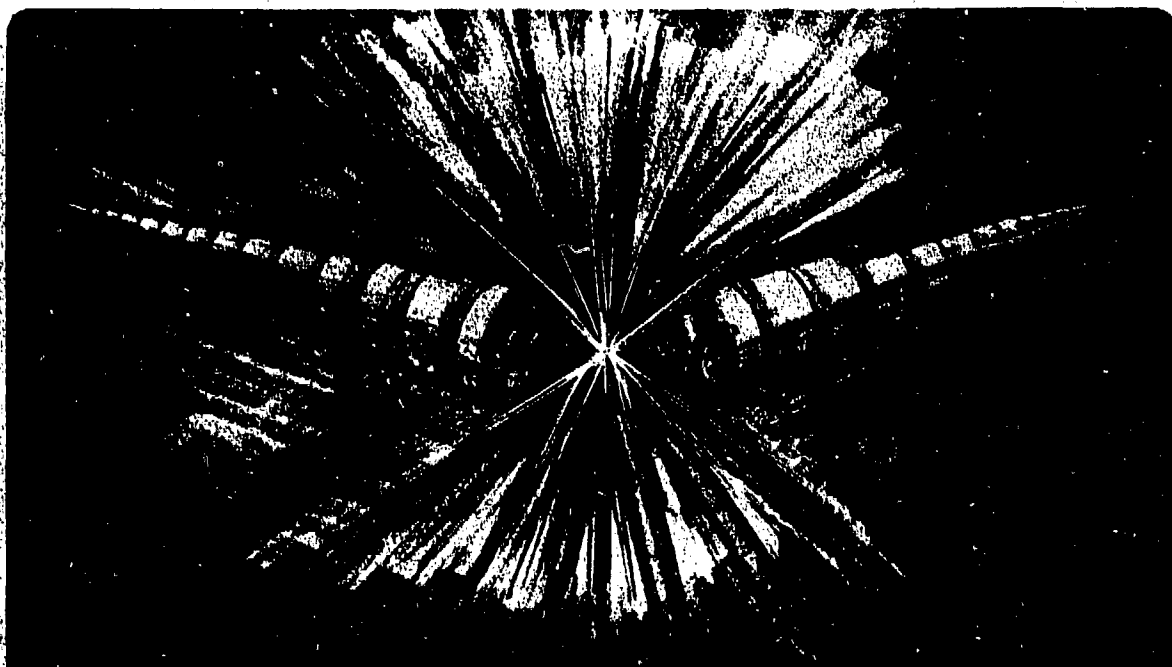
LBL--22228

VARIED-SPACE GRAZING INCIDENCE GRATINGS IN HIGH RESOLUTION SCANNING SPECTROMETERS

DE87 002568

M.C. Hettrick and J.H. Underwood

October 1986



Prepared for the U.S. Department of Energy under Contract DE-AC03-76SF00098

DISTRIBUTION OF THIS DOCUMENT IS UNLIMITED

LEGAL NOTICE

This book was prepared as an account of work sponsored by an agency of the United States Government. Neither the United States Government nor any agency thereof, nor any of their employees, makes any warranty, express or implied, or assumes any legal liability or responsibility for the accuracy, completeness, or usefulness of any information, apparatus, product, or process disclosed, or represents that its use would not infringe privately owned rights. Reference herein to any specific commercial product, process, or service by trade name, trademark, manufacturer, or otherwise, does not necessarily constitute or imply its endorsement, recommendation, or favoring by the United States Government or any agency thereof. The views and opinions of authors expressed herein do not necessarily state or reflect those of the United States Government or any agency thereof.

**VARIED-SPACE GRAZING INCIDENCE GRATINGS IN
HIGH RESOLUTION SCANNING SPECTROMETERS**

Michael C. Hettrick and James H. Underwood

**Center for X-ray Optics
Lawrence Berkeley Laboratory
University of California
Berkeley, California 94720**

October 1986

Published in "Short Wavelength Coherent Radiation: Generation and Applications" Monterey, CA March 1986. D.T. Attwood and J. Bokor, Eds. (AIP Conf. Proc. 147).

**This work was supported by the Office of Basic Energy Sciences,
U.S. Department of Energy, under Contract # DE-AC03-76SF00098.**

MASTER

**VARIED-SPACE GRAZING INCIDENCE GRATINGS IN
HIGH RESOLUTION SCANNING SPECTROMETERS**

Michael C. Hettrick and James H. Underwood

**Lawrence Berkeley Laboratory
Center for X-ray Optics
Berkeley, California 94720**

ABSTRACT

We discuss the dominant geometrical aberrations of a grazing incidence reflection grating and new techniques which can be used to reduce or eliminate them. Convergent beam geometries and the aberration correction possible with varied groove spacings are each found to improve the spectral resolution and speed of grazing incidence gratings. In combination, these two techniques can result in a high resolution ($\lambda/\Delta\lambda > 10^4$) monochromator or scanning spectrometer with a simple rotational motion for scanning wavelength or selecting the spectral band.

INTRODUCTION

The increased demand for intense, coherent sources of soft x-ray and extreme ultraviolet radiation¹ motivates the development of new spectroscopic instruments operating in the grazing incidence regime $\lambda = 10\text{-}1000 \text{ \AA}$. X-ray holography,^{2,3} photoelectron spectroscopy⁴ and grating microscopy^{2,5} all require a pre-monochromator with spectral resolving power $\lambda/\Delta\lambda = 10^3 - 10^4$ and higher. For example, at a wavelength of 30 \AA , a coherence length of 60 microns converts to a resolving power of approximately 2×10^4 .

Existing spectroscopic instruments are not capable of delivering such high performance without severely compromising other requirements. For example a conventional Rowland circle grating, constrained to the geometry of equidistant grooves, results in considerable astigmatism, an oblique spectrum, and complicated motions for scanning wavelength⁶. In applications where only low or modest spectral resolution is required ($\lambda/\Delta\lambda < 10^3$), the spherical grating surface can be replaced by a toroid⁷, resulting in a near removal of astigmatism. Visible holography can also be used to alter the focal surface of spectra and to improve the imaging⁸. However, each of these techniques is severely limited in its potential for dramatic aberration correction at short wavelengths.

During the past several years, a new technique in grating fabrication has emerged as a demonstrated tool for aberration correction. Ruling engines outfitted with state-of-the-art interferometric readout systems and computer control have made it possible to vary the spacings of grooves in a continuous

manner across the grating ruled width^{9,10}. This technological advance has been successfully exploited in the field of soft x-ray and extreme ultraviolet spectroscopy, providing erect focal surfaces for imaging of spectra^{9,11} at high resolution. Curved grooves have also been recently demonstrated with a mechanical ruling engine¹⁰. With these new degrees of freedom it is now possible to first specify the desired performance, and then to deduce the mechanical ruling corrections necessary to yield these characteristics. This is a reversal of the situation confronted by grating scientists since the time of Rowland.

In addition to new groove patterns, the use of unconventional beam geometries has allowed the use of simple optical surfaces. A plane grating surface placed in convergent incident light has been shown to provide imaging free of astigmatism¹². Such a geometry is particularly convenient in space-borne instruments, due to the presence of a large telescope for collection of the incident light. This not only increases the effective speed of the optical system, but also employs a simple optical surface which can be made to the accuracy required for high resolution.

The purpose of this paper is to apply the principles of varied spacing and simple (plane or spherical) grating surfaces to the task of designing grazing incidence laboratory monochromators. We indicate the design options available today and in the near future for the construction of high spectral resolution monochromators and scanning spectrometers. We emphasize the potential of an advanced varied space grating to maintain high resolution ($\lambda/\Delta\lambda > 10^4$) over a wide wavelength region through a simple rotational scanning motion, particularly convenient in the environment of an ultra-high vacuum.

THE LIGHT-PATH FUNCTION

In the short wavelength domain, below approximately 1000 Å, the physical diffraction-limited resolution of most optics is insignificant and the main task is the minimization of its geometrical aberrations. The analytical formalism which is most instructive for the purpose of understanding the geometrical aberrations of a diffraction grating is based on Fermat's principle. It states that a light ray will trace a path through an optical system so as to minimize variations in its effective path-length. The effective path-length, F , equals the physical length traversed, L , minus the phase shift of grating groove N :

$$F(w, \ell) = L(w, \ell) - m\lambda N(w, \ell) \quad (1)$$

where L and N are each functions of the position (w, ℓ) at which the light ray strikes the optical aperture. If a normal incidence focal plane is placed a distance r' from the grating center, then Fermat's principle can be used to find the focal position (x, y) :

$$x \approx r' dF/dw / \cos\beta, \quad y \approx r' dF/d\ell \quad (2)$$

where β is the angle made with the grating surface normal by the ray as it is diffracted, and x is in the direction of spectral dispersion. Equation 2 indicates the ray positions at which maximum constructive interference is achieved for light diffracted from the immediate vicinity of grating

coordinate pair (w, ℓ) . Given a finite grating size, x and y will drift over a range of values, resulting in an image whose size represents the total geometrical aberration of the optic.

When the grating sizes w and ρ are small in comparison to the object distance r , it is useful to expand the light-path function as a power series in these grating coordinates:

$$F(w, \ell) = \sum F_{ij}(w, \ell) w^i \ell^j \quad (3)$$

$$\text{where } F_{ij}(w, \ell) = L_{ij}(w, \ell) - m\lambda N_{ij}(w, \ell). \quad (4)$$

In the case of a spherical surface with radius R the path-length coefficients, L_{ij} , are well known¹³:

$$L_{00} = r + r' = \text{length of the principal ray;}$$

$$L_{10} = \sin \beta - \sin \alpha;$$

$$L_{20} = \frac{1}{2} \left(\frac{\cos^2 \alpha}{r} - \frac{\cos \alpha}{R} \right) + \frac{1}{2} \left(\frac{\cos^2 \beta}{r'} - \frac{\cos \beta}{R} \right)$$

$$L_{02} = \frac{1}{2} \left(\frac{1}{r} - \frac{\cos \alpha}{R} \right) + \frac{1}{2} \left(\frac{1}{r'} - \frac{\cos \beta}{R} \right)$$

$$L_{30} = - \frac{\sin \alpha}{2r} \left(\frac{\cos^2 \alpha}{r} - \frac{\cos \alpha}{R} \right) + \frac{\sin \beta}{2r'} \left(\frac{\cos^2 \beta}{r'} - \frac{\cos \beta}{R} \right)$$

$$L_{12} = - \frac{\sin \alpha}{2r} \left(\frac{1}{r} - \frac{\cos \alpha}{R} \right) + \frac{\sin \beta}{2r'} \left(\frac{1}{r'} - \frac{\cos \beta}{R} \right)$$

... and higher-order terms. (5)

The coefficients a_n associated with the interference term (N_{ij}) are dependent on the distance between adjacent grooves (σ) and on the groove

pattern (linear, circular, elliptical, etc). Following Harada & Kita⁹ we expand the groove density as a power series in w along the mid-plane of the grating ($l = 0$):

$$1/\sigma = 1/\sigma_0 + a_1 w + a_2 w^2 + a_3 w^3 + \dots \quad (6)$$

where the coefficients a_n provide the effect of varied spacing. Thus, for the otherwise classical case of straight grooves formed at the intersection of the grating spherical surface and parallel planes oriented normal to this surface at the grating pole ($w = 0$), we have:

$$N_{10} = 1/\sigma_0; \quad N_{20} = a_1/2, \quad N_{30} = a_2/3 \quad (7)$$

It should be noted that only the interference term N_{10} is present for conventional equally spaced grooves, and varied spacing itself effects the aberration terms dependent only on w . Aberration correction of terms involving the groove length l (dominant F_{02} and F_{12}), requires groove curvature. In the case of a spherical surface, Harada and Kita have shown that a conventional rectilinear ruling motion can supply a small amount of groove curvature by tilting the ruling planes relative to the grating normal at its center⁹. The groove curvature radius obtained with this technique is approximately $R/\tan\theta$ as viewed from the grating normal, where θ is the ruling plane tilt which can be as large as 30° . An even more direct means of obtaining groove curvature has been developed by Hirst, being a "circular ruling engine"¹⁰. This makes it possible to rule concentric grooves with a maximum radius of curvature of approximately 500 mm, independent of the

grating surface shape. These radii are typically much shorter than obtained with the technique of Harada, and thus the two methods complement each other. If the distance from the grating center to the groove rotation axis is D_0 , then one can derive the aberration correction coefficients N_{ij} by the substitution $w = D_0 - \sqrt{(D_0 - w)^2 + l^2}$ in equation (6). In particular, this results in non-zero values for N_{02} (astigmatism correction) and N_{12} (astigmatic coma correction). However, in the discussion which follows, we consider only varied-space straight grooves.

LINE PROFILES

Ideally, the path-lengths (equation 5) and their interference shifts (equation 7) would cancel each other, resulting in individual terms $F_{ij} = 0$.

Such a system images a point source without aberration, and is referred to as stigmatic. Of course, this is difficult to realize in any practical optical system, and one must consider the effect of various aberrations. Apart from the term F_{10} , which via the grating equation is zero, each aberration will produce a point-spread function of the image at the focal plane. For example, in the direction of dispersion,

$$dI/dx = c x^{(2-i)/(i-1)} \quad (8)$$

where I is the intensity and c is a normalization factor. In Fig. 1 we sketch the image profiles for non-zero values of F_{20} ($i = 2$), F_{30} ($i = 3$) and F_{40} ($i = 4$). These images are distinguishing in shape, and are usually referred to as "de-focusing" ($i = 2$), "coma" ($i = 3$) and "spherical

aberration" ($i = 4$) by grating designers. Similar aberrations are in general present in the perpendicular direction, y , along the height of the image, the first of these being "astigmatism" ($j = 2$).

CLASSICAL SCANNING ABERRATIONS

In the classical case of a spherical grating with equidistant straight grooves, both de-focusing and coma are absent along the Rowland circle. The image shape is dominated in the dispersion direction by spherical aberration and in the image height direction by considerable astigmatism. The situation worsens quickly when one deviates from the Rowland circle at grazing incidence. For example, given an immovable source and exit slit, a convenient rotation of the grating about its pole is commonly used to scan wavelength, such as used in a conventional toroidal grating monochromator⁷. However given the classical ruling constraint $a_n = 0$, equations 5 and 7 reveal there is only enough freedom to independently choose r and r' , and thus to remove the de-focusing aberration (F_{20}) at two wavelengths. In Fig. 2 we show the spectral resolution due to the de-focusing term as a function of wavelength for a 1500 g/mm grating with 20 meter radius of curvature, a focal length r' of approximately 2.5 meters, a graze angle of approximately 9° , a numerical aperture of 0.02 and an angular deviation of 162° . The optimum wavelengths are 150 Å and 250 Å, away from which the aberration grows rapidly, resulting in an average spectral resolution of only 300 over the 100-300 Å band. This is a factor of 10-100 smaller than desired for future high-resolution studies.

VARIED-SPACE PLANE GRATING

This geometry is illustrated in Fig. 3, and has been previously discussed in the context of extreme ultraviolet spectroscopy^{12,14,15}. The grating surface is flat, and operates in a light beam converging to a point focus. We consider the use of straight grooves for which the astigmatism term vanishes if the virtual source and real focus are equal distances from the central groove of the grating. In such a mounting, the amount of astigmatic coma (F_{12}) is very small. Setting $r = -r'$ in equation 5, we find this aberration limits the spectral resolving power to^{14,15}:

$$\lambda/\Delta\lambda = 8f_y^2, \quad (9)$$

where f_y is the beam speed along the grooves. In contrast to most gratings, this result is independent of the graze angle. For example, in a typical laboratory or synchrotron configuration with $f_y = 50$, the resolving power is 20,000. For a comparable soft x-ray toroidal grating, astigmatic coma limits the resolution to approximately $\lambda/\Delta\lambda = 11$; even with the use of a correcting toroidal mirror in tandem, the spectral resolution would be only approximately 275 for an optimized toroidal grating monochromator⁷. Thus, as an astigmatism-free device, it appears that a plane grating in convergent light far outperforms the available alternatives. A derivative of this design, in which the light converges only in the groove length direction of a cylindrical grating, would have the same low level of sagittal coma, which at

grazing incidence can be approximately recovered by a spherical surface.¹⁶

By use of varied spacing, all of the in-plane aberrations F_{n0} can be eliminated at one wavelength of choice. This can be seen by adjustment of the coefficients a_n in equations 6 and 7, or by inversion of the grating equation¹⁴ to determine the local spacing required at coordinate w . With these corrections, the grating is free of astigmatism, nearly free of astigmatic coma, and free of all aberrations along the mid-plane ($l = 0$). In addition to this quasi-stigmatism, the focal surface for imaging of a spectrum is at normal incidence relative to the diffracted beam, resulting from the fact that both the chosen wavelength and the zero order image are at equal distances from the grating center.

We now consider adopting this geometry for a monochromator, and scan wavelength by simply rotating the grating about its central groove, keeping the source and exit slit fixed. In Fig. 2 we show the increase in the de-focusing aberration (F_{20}) away from a corrected wavelength of 200 Å. Over a scanning region of approximately 30 Å, the spectral resolving power is kept better than 10,000. This insensitivity to small rotations of the grating has been previously noted in the context of a misalignment aberration¹⁵:

$$\lambda_* / \Delta\lambda_* = \tau_y (\cos \beta_* / \cos \alpha_* - 1) / f_x \quad (10)$$

where f_x is the focal speed of the grating across its ruled width, τ_y is the rotation angle for selection of wavelength, and λ_* is the quasi-stigmatic wavelength.

MODIFICATIONS TO THE BASIC DESIGN

This performance can be significantly enhanced by a slight relaxation of two assumptions which have been made in the design of space instruments based on this varied-space grating^{12,14,15}:

a) The flat grating surface provides a stigmatic zero order image in reflection, which facilitates alignment and wavelength calibration of a spectrum. However, by curvature of the grating surface the defocusing aberration of a second wavelength (i.e. in addition to λ_x) can be removed. This is particularly useful in extending the usable scanning range of a monochromator. Due to the use of converging incident light, the required deviation from flatness is extremely small, typically corresponding to hundreds of meters in radius. Optimally, this radius could be obtained by use of a cylindrically bent grating substrate, for which equation 9 still holds and astigmatic coma thereby remains small. However, with such large radii, the sagittal focusing is in practice negligible, allowing the use of a spherical grating in most circumstances.

b) The use of converging incident light onto the grating requires a fore-optic to refocus the entrance slit or source. In space astronomy, this is provided automatically by a large aperture telescope required in any event to collect the starlight. Such telescopes typically provide a single focus, which leads to the requirement of $r = -r'$ in order to remove astigmatism. However, by using a Kirkpatrick-Baez (K-B) mirror system¹⁷ in a laboratory instrument, the focal distances in the two orthogonal directions can be made unequal. This allows the virtual distance r to take on two values: r_t in

the plane of reflection and r_s along the grooves. By setting $-r_s$ equal to the grating focal distance r' , astigmatism will still be removed and equation 9 still valid. This leaves a free parameter, r_t , which can be used for further aberration correction. We find the most powerful such adjustment to be a removal of the derivative $dF_{20}/d\tau_y$ at one of the two wavelengths where F_{20} has also been set equal to zero¹⁸. In combination with a finite radius of curvature, this leads to the following focusing condition:

$$r_t/R = (t_2 s_1 - t_1 s_2)/(t_2 u_1 - t_1 u_2) \quad (11)$$

$$r'/R = -r_s/R = t_1/(u_1 - s_1 R/r_t) \quad (12)$$

where the constants are:

$$\begin{aligned} s_n &= -\cos^2 \alpha_n (\cos \alpha_n + \cos \beta_n) + 2\cos \alpha_n \sin \alpha_n (\sin \beta_n - \sin \alpha_n) \\ t_n &= -\cos^2 \beta_n (\cos \alpha_n + \cos \beta_n) - 2\cos \beta_n \sin \beta_n (\sin \beta_n - \sin \alpha_n) \\ u_n &= -2(1 - \sin \alpha_n \sin \beta_n + \cos \alpha_n \cos \beta_n) \end{aligned} \quad (13)$$

and where the defocusing term vanishes at wavelengths λ_n ($n = 1, 2$). The derivative of the defocusing term will also vanish at correction wavelength λ_1 .

The dot-dash curve in Fig. 2 shows the result of applying these fine aberration corrections assuming the same basic parameters as before (1500 g/mm, 162° angular deviation, $r' = 2.5$ m, 9° graze angle and a numerical aperture of 0.02). The de-focusing vanishes at 150 Å and 250 Å, rising to only approximately 10^{-5} between these wavelengths. Higher order scanning aberrations (e.g. F_{30}, F_{40}) must also be considered, but these can be made zero at one wavelength and decrease as the square and higher powers of the

numerical aperture.

In Fig. 4 we illustrate one possible optical configuration consistent with the optimized design discussed above. As the grating accepts a large numerical aperture (0.02), the entrance slit would be fed by a single mirror which de-magnifies the source size (e.g. synchrotron radiation) in the dispersion direction, thus providing high spectral resolution. A system of two bent glass or bent metal mirrors^{19,20} in an orthogonal (K-B) arrangement provides a convergent beam to the grating. The bent mirror approach results in cylindrical optical surfaces for which the imaging in each direction is de-coupled, and thus absent of the mixed aberrations which dominate a single aspherical mirror. The mirror M1 refocuses the entrance slit to an optimum point V behind the grating, whereas M2 images the original source onto the exit slit in the direction perpendicular to dispersion. Over selected bandpasses, the K-B re-focusing system can be replaced by a single spherical mirror operated off-axis to form the two desired foci. Using the numerical ray trace program SHADOW (developed by F. Cerrina), we have verified the expected quasi-stigmatic imaging property of an entire spectroscopic system of this type. With a 100 micron wide entrance slit, a spectral resolution of 12,500 was obtained for a plane varied-space grating at a wavelength of approximately 200 Å. The point source response represented a resolution of 30,000 limited by astigmatic coma, and an image height of 30 microns. The variation in groove spacing required is only 20%, easily accommodated with existing numerically controlled ruling engines^{9,10}. For the widest bandpass during scanning, a grating curvature radius of 500 meters would be used.

Advantages of the proposed monochromator design are as follows:

- 1) No astigmatism;
- 2) Small astigmatic coma;
- 3) Simple rotational motion for selecting wavelength;
- 4) Negligible scanning aberrations over a wide spectral band;
- 5) Straight groove pattern on a plane or spherical grating surface;
- 6) Erect focal surface for use as a spectrometer;

We thank F. Cerrina for use of the ray trace program SHADOW, and modifications executed to permit varied-space mechanical rulings. We are aware of other related work being done in this area, including the use of a holographically recorded grating to construct a monochromator with similar properties to those discussed above²¹. This work was supported by the Office of Basic Energy Sciences, U.S. Department of Energy, under Contract No. DE-AC03-76SF00098.

REFERENCES

1. D. Attwood, K. Halbach and K.-J. Kim, *Science* 228 , 1265 (1985).
2. M. Howells and J. Kirz, AIP Conf. Proc. No. 118 on Free Electron Generation of Extreme Ultraviolet Coherent Radiation, ed. by J.M.J. Madey and C. Pellegrini, (Amer. Inst. Phys., New York, 1983), p. 85.
3. P.L. Csonka, *J. Appl. Phys.* 52, 2692(1981).
4. M.O. Krause, in Synchrotron Radiation Research, ed. by H. Winick, (Plenum Press, 1980), p. 101.
5. M.C. Hettrick, Aplanatic Grazing Incidence Diffraction Grating, *Appl. Opt.* 25, 3269 (1986).
6. S.L. Hulbert, J.P. Stott, F.C. Brown and N.C. Lien, *Nucl. Instrum. Meth.* 208, 43(1983).
7. C.T. Chen, E.W. Plummer and M.R. Howells, *Nucl. Instrum. Meth.* 222, 103(1984).
8. R.J. Fonck, A.T. Ramsey, and R.V. Yelle, *Appl. Opt.* 21, 2115 (1982).
9. T. Harada and T. Kita, *Appl. Opt.* 19, 3987 (1980).
10. G. E. Hirst, *Proc. Soc. Photo-Opt. Instrum. Eng.* 560, 46 (1985).
11. M.C. Hettrick, S. Kahn, W.R. Craig and R. Falcone, Varied line space grating spectrometer for x-ray transfer experiments in optically thick plasmas, (in preparation, 1986).
12. M.C. Hettrick, S. Bowyer, R. Malina, G. Martin and S. Mrowka, *Appl. Opt.* 24, 1737 (1985).
13. T. Namioka, *J. Opt. Soc. Am.* 49, 446 (1959).
14. M.C. Hettrick and S. Bowyer, *Appl. Opt.* 22, 3921 (1983).

References page 2

15. M.C. Hettrick, Appl. Opt. 23, 3221 (1984).
16. M.C. Hettrick and J.H. Underwood, Stigmatic High Throughput Monochromator (HTM) for Soft X-rays, Appl. Opt. accepted (1986).
17. P. Kirkpatrick and A.V. Baez, J. Opt. Soc. Am. 38, 766 (1948).
18. Aberration correction of a rotational mounting has been discussed for the case of normal incidence by R. Iwanaga and T. Oshio, J. Opt. Soc. Am. 69, 1538 (1979).
19. J.H. Underwood and D. Turner, Proc. Soc. Photo-Opt. Instrum. Eng. 106, 125 (1977).
20. Acton Research Corporation, Acton, MA 01720. Model AMA-250.
21. M. Pouey, Proc. Soc. Photo-Opt. Instrum. Eng. 597, 64 (1985).

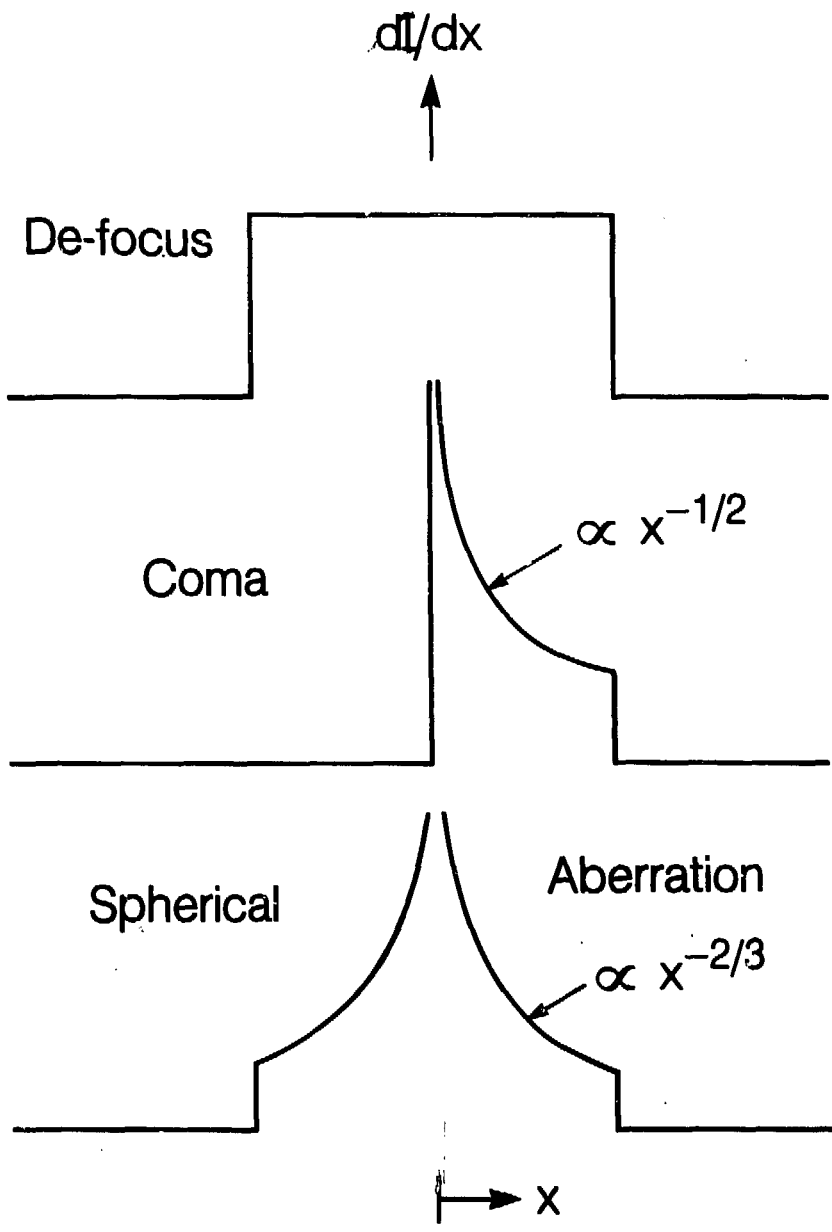
FIGURES

Fig. 1. Line profiles of ray aberrations at a focal plane. The vertical direction is proportional to the intensity of photons diffracted per unit displacement in the dispersion direction (horizontal). De-focusing (top) yields a uniform intensity whereas coma (middle) and spherical aberration (bottom) are peaked at the ray position from the grating center. Extremum image size is defined by the sharp edges corresponding to rays diffracted from the grating width edges. The dominant aberration in magnitude of extremum width, if left uncorrected, would be de-focusing.

Fig. 2. Fractional resolution versus wavelength, scanned with a simple rotation of the grating about its central groove, using fixed entrance and exit slits. Only the de-focusing aberration is plotted here (F_{20} in text). A spherical or toroidal grating with equally spaced grooves (solid) is compared to a varied-space plane grating (dashed) and an improved version where the radius of grating curvature is large, and the de-focusing term is stationary at 150 Å.

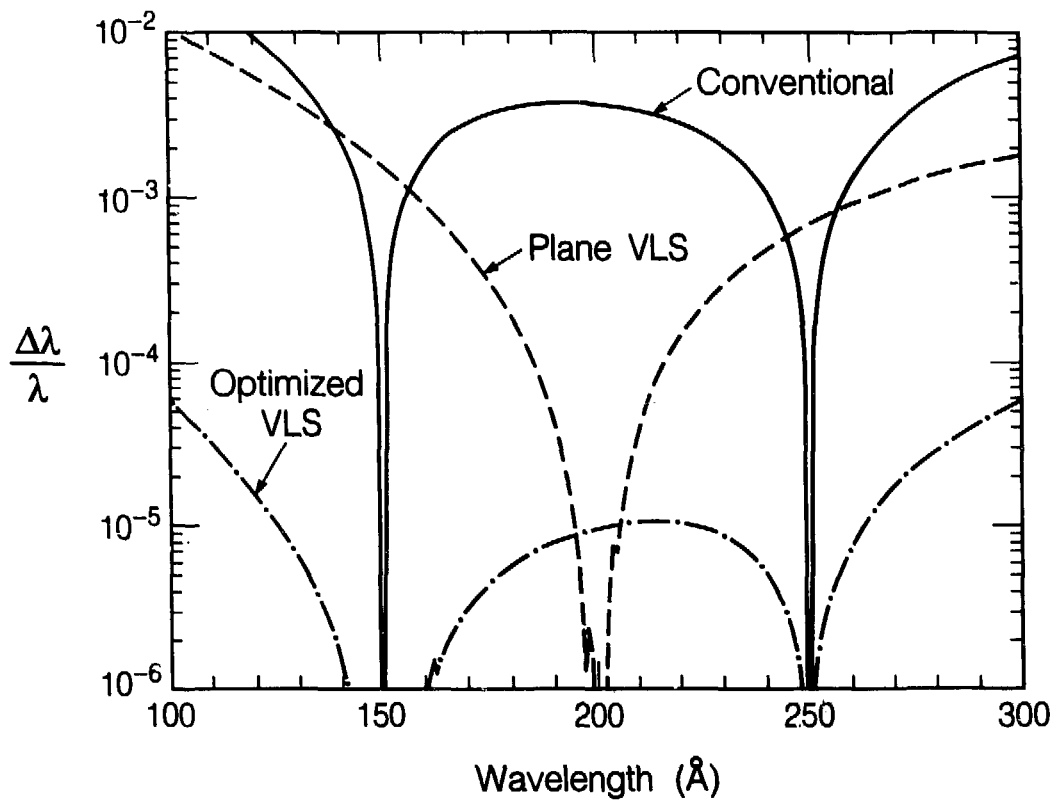
Fig. 3. Geometry of a varied space plane grating in convergent light. One wavelength of choice in addition to zero order is stigmatic along the astigmatism-free focal surface shown here. The residual aberration at this wavelength is sagittal coma, also called "astigmatic" coma, which depends on the square of the sagittal focal speed f_y . Lower panel shows the grating plane, containing straight grooves.

Fig. 4. High resolution grazing incidence monochromator. An approximately planar grating in convergent light can be rotated to select wavelength with minimum aberration. The re-focuser can be replaced by a normal incidence spherical multilayer placed offaxis.



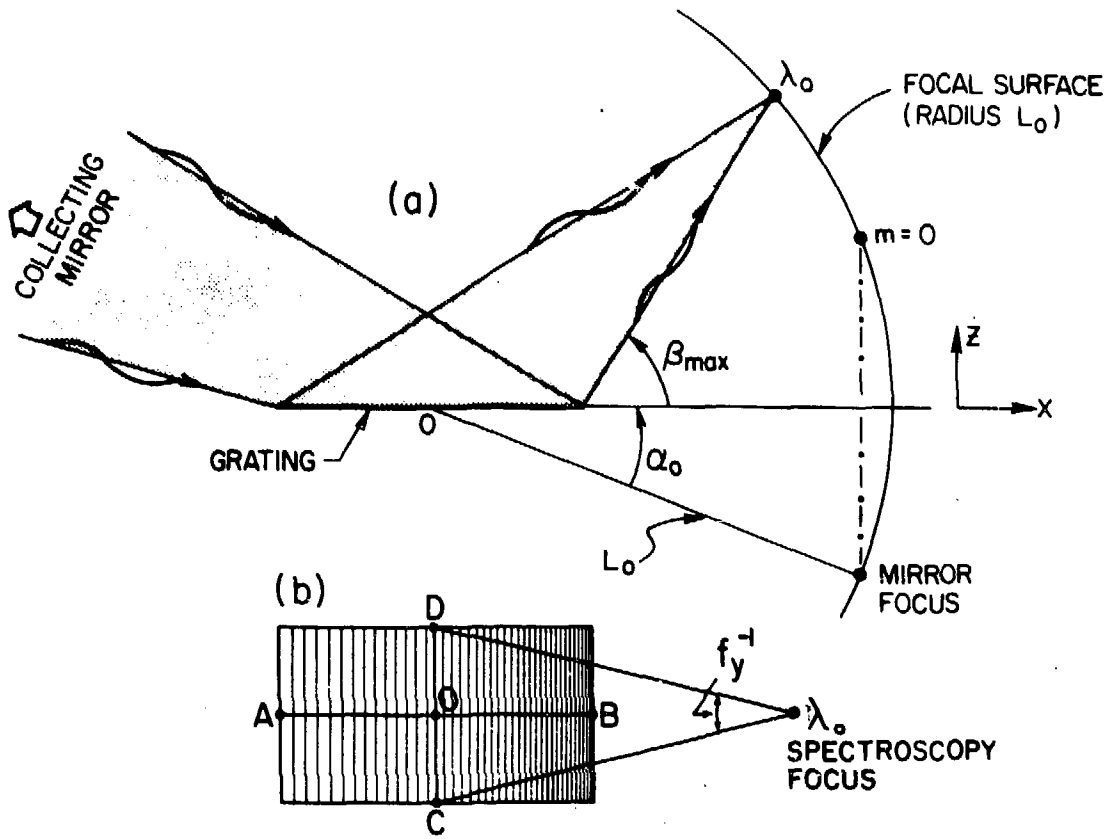
XBL 863-9777

Figure 1



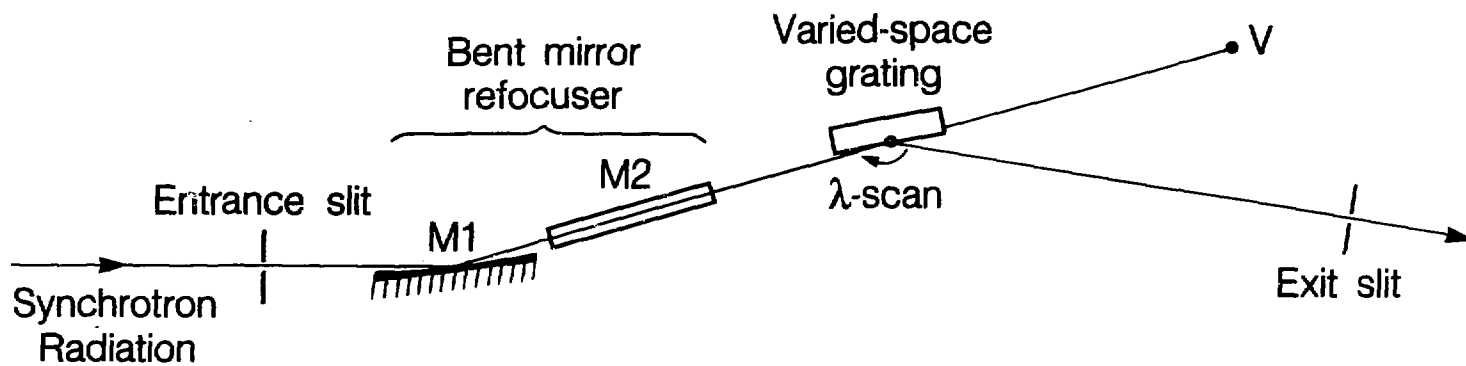
XBL 863-9779

Figure 2



XBL 8610-3681

Figure 3



XBL 863-9778

Figure 4

This report was done with support from the Department of Energy. Any conclusions or opinions expressed in this report represent solely those of the author(s) and not necessarily those of The Regents of the University of California, the Lawrence Berkeley Laboratory or the Department of Energy.

Reference to a company or product name does not imply approval or recommendation of the product by the University of California or the U.S. Department of Energy to the exclusion of others that may be suitable.